Hindawi
Shock and Vibration
Volume 2018, Article ID 1098531, 13 pages
https://doi.org/10.1155/2018/1098531

Research Article

Analysis of Vibration Reduction by Damping Using Simple Analytical Modelling

Goran Pavić

Vibration-Acoustics Laboratory, INSA, Villeurbanne 69621, France

Correspondence should be addressed to Goran Pavić; goran.pavic@insa-lyon.fr

Received 20 February 2018; Accepted 20 May 2018; Published 14 June 2018

Academic Editor: Gabriele Cazzulani

The performance of different solutions to global vibration reduction using external damping is discussed. The solutions are either uneven distribution of structural damping or use of vibration absorbers. To this end, a comparative study is carried out, built on simple analytical models. It is shown that a well-chosen solution can produce a substantial reduction of global vibration level. It is further shown that the overall damping effect critically depends on the mutual interaction between the applied damping device and the damped structure. Qualitative guidelines are provided about the selection of appropriate parameters that affect damping performance.

1. Introduction

Vibration damping is considered to be effective only under resonant vibration conditions of an elastic structure. The frequency response of a single-degree-of-freedom system driven by a force well illustrates this feature. From a design perspective, the damping is taken as a remedy to high vibration levels if (a) the excitation is stationary and localised to frequencies close to system resonances or if (b) the vibration is of transient nature. Where vibration modelling is concerned, the damping is generally not considered as a major difficulty. By employing the notion of structural damping, the energy dissipation within an elastic structure is often expressed by a loss factor η equal to the ratio of irreversible and reversible energy of vibration [1]. In the case of harmonic motion, this is accounted for by simply attributing to elastic constants an imaginary part proportional to η. In most cases, a unique η is applied to a given system; typical modelling value is 0.01 (1%).

While the damping of a simple resonator is indeed effective only close to its (unique) resonant frequency, a complex system of high overlap of resonances will be sensitive to damping across a broad frequency range. In such a case, the way the damping is distributed across the system can influence significantly the system response.

In this paper, a simple analysis will be carried out with the goal of investigating how the amount of damping and the way it is distributed affect the vibration level of a structure. For the sake of clarity, a smooth frequency power law of excitation is assumed, that is, flat or linear. In the absence of any specific objective regarding the location of vibration response, the global vibration will be considered, represented by the kinetic energy of the concerned part of the analysed system. Modelling will be done analytically in order to make the comprehension of underlining physics easier.

2. Uneven Damping Distribution

To start with, take a simple mass-spring oscillator with hysteretic damping excited by a force of uniform power spectral density G_F. Its kinetic energy T can be computed using the Residue Theorem. The energy is inversely proportional to the product $\eta\sqrt{km}$ where, η is loss factor, k is stiffness, and m is mass:

$$T = \frac{G_F}{8\eta\sqrt{km}} \tag{1}$$

The factor $\sqrt{km}$ will be named the "resistance" of the oscillator; its dimension is that of ordinary force/velocity

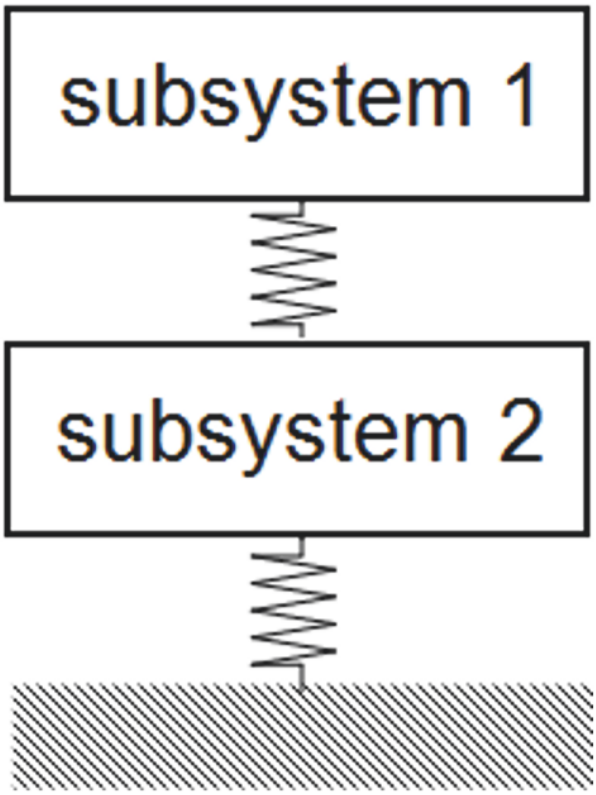

Figure 1: Simple two-DOF system.

impedance. It follows that, under a given excitation, the energy of a wideband-excited oscillator can be reduced by increasing either its damping or its resistance. These two quantities, the loss factor and the resistance, will be further used as the distinctive features of a particular oscillator or a particular degree of freedom appearing in the analysis.

2.1. Two Simple Subsystems. In this section, two basic mechanical configurations will be analysed. To keep the analysis simple, it will be considered that the motion is a pure translation and that it occurs in a single direction only. Each of the configurations will be modelled as a two-degrees-of-freedom system composed of two subsystems as shown on Figure 1. More complex modelling at this stage would hinder the analysis in that it would involve too many independent parameters, thus making it impossible to draw generic conclusions.

The first configuration is representative of a vibrating machine elastically suspended to a resonant support. In this case, subsystem 1 is the source, that is, the machine, together with the first stage of suspension modelled as a spring. Subsystem 2 is the support, that is, the frame with the second stage of suspension. The excitation is provided by a force acting on the source, that is, on the mass of subsystem 1.

The second configuration is typical of equipment suspended to a vibrating housing. While the architecture of two subsystems remains the same as in the first case, the difference is in the excitation. The latter is now provided by the ground motion and is transmitted to the mass of subsystem 1 via suspension springs 2 and 1.

In either of the two cases, the dissipation is accounted for by assuming that the suspension springs possess hysteretic damping. The mathematical model of the system and the computation of total kinetic energy are given in Appendix A.

The system shown possesses six independent parameters: mass, stiffness, and loss factor of each of the two subsystems. While a single-degree-of-freedom oscillator is fully defined in terms of its resistance and loss factor, where broadband frequency excitation is concerned, the present system will need another descriptor that governs its response: the position of eigenfrequencies of the two subsystems. Bearing this in mind, the system's parameters will be here recomposed in the following nondimensional form: r is the ratio of the resistances of the support and the source, $r = \sqrt{k_2 m_2 / k_1 m_1}$, and e is the ratio of the uncoupled eigenfrequencies of the support and the source, $e = \sqrt{k_2 m_1 / k_1 m_2}$. Together with the two loss factors, η_1 and η_2, these parameters will provide the basis for a comparative analysis of damping effects.

The basic features of 2-DOF oscillators driven via the base motion of uniform spectrum have been analysed in [2]. The system response was found to be increasingly sensitive to the values of its parameters if the uncoupled natural frequencies were of the same order. In [3], the authors have found that the mass ratio of the two subsystems inferior to 0.1 produces the system response very sensitive to this ratio, depending on system parameters in a rather complicated way. Quite surprisingly the "no-loading" approximation has been used to enable a simplified computation of the global response of the subsystems. The results did not reveal any particular dependence of vibration levels on system parameters, which could be exploited as design guidelines.

In what follows, the analysis of the system vibration will be done with no approximations and using much larger scope of parameter values than previously done. Each of the four nondimensional system parameters r, e, η_1, and η_2 was assigned 9 different values and all of possible 6561 combinations of subsystem kinetic energies integrated over the frequency band $(0, \infty)$ were evaluated. The 9 values of r and e parameters spanned in logarithmic fashion from 0.2 to 5 and from 0.2% to 5% for either of the two loss factors. The results were then normalised using the mean of respective kinetic energies taken over all of computed combinations. The normalisation has thus provided a simple means to judge the relative impact of a particular combination of parameters to the global vibration level.

Figure 2 gives the normalised kinetic energy as a function of input parameters relative to the upper subsystem (left), lower subsystem (middle), and the entire system (right). One hundred lowest and one hundred highest energy values are shown, face to face with the corresponding values of four system parameters. The latter are presented by a 9-level grey scale. The top plots refer to force excitation of upper subsystem, while the bottom ones refer to the acceleration excitation of system base. Blue curve and lower scale refer to lowest energy levels; red curve and upper scale refer to highest energy levels.

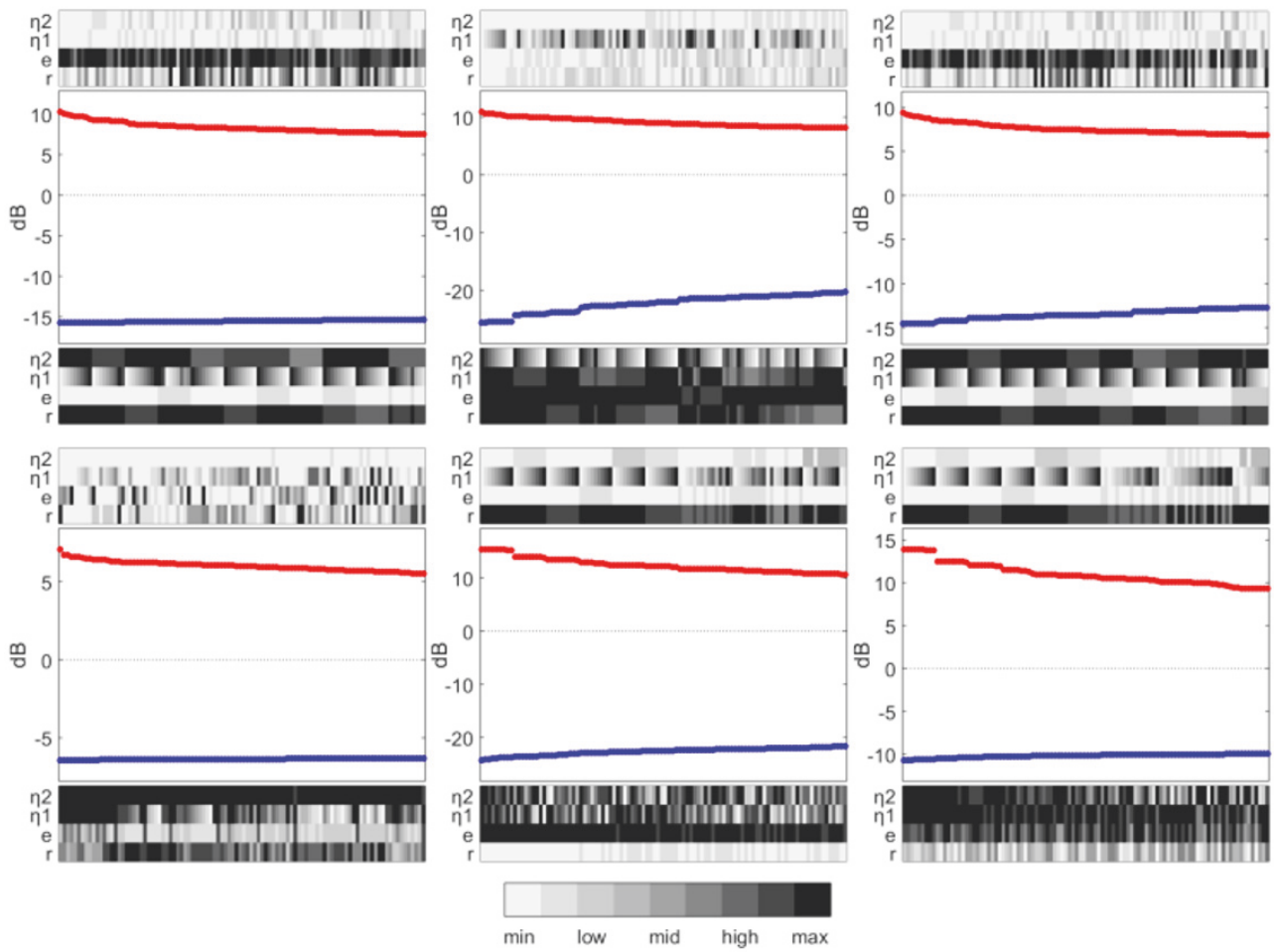

Figure 2: Normalised kinetic energy levels of a two-degrees-of-freedom system. Top: force excitation; bottom: kinematic excitation. Left: subsystem 1; middle: subsystem 2; right: entire system.

Since the results cover different combinations of system parameters with relatively fine resolution, it can be assumed that generality is satisfied. Several broad conclusions can be thus drawn from the figures.

Regarding force-driven upper subsystem, that is, source driving the support, increasing the resistance ratio r lowers the vibration of both the source and the support. Provided that this condition is met, further lowering of source vibration can be achieved by making e low, that is, by stiffening source suspension. Adding support damping helps reduce source vibration, while no major effect is produced by increasing source damping. On the other hand, softening the source suspension makes the source level increase. This, however, helps reduce the vibration level of the support as does moderate increase of source damping. On the contrary, lowering of r and e as well as reducing the support damping increases the vibration of support.

Regarding base-driven lower subsystem, that is, housing driving the equipment, by maximizing the housing damping, the vibration of the equipment is halved provided that the natural frequency of the housing is lower than that of the equipment. Large mismatch in resistances and high housing resonant frequency, that is, low r and high e, lead to reduction of housing vibration. On the contrary, large values of r and low values of e result in increase of housing vibration. Low damping of housing is detrimental to vibration of both housing and equipment, while damping of the equipment does not seem to play any major role in vibration reduction.

The r and e ratios can be considered as main design parameters of a given assembly, as these involve the mass and stiffness of subsystems. Further analysis was made by varying these two parameters in the sequence 0.2-0.5-1-2-5 and by averaging the kinetic energies over all combinations of loss factors of the two subsystems within the range 0.002–0.05. The results shown in Figure 3 give the kinetic energy level for each r-e pair, normalised to the corresponding kinetic energy average. Shown from left to right are the matrix plots of the normalised energy levels of subsystem 1, subsystem 2, entire system, and entire system subjected to equivalent uniform damping, respectively. The latter was represented by a unique loss factor obtained by resistance-weighted average of η_1 and η_2. The top row refers to force-driven subsystem 1; the bottom row refers to base-driven subsystem 2.

Table 1: Damping-averaged vibration level. Top: force-driven subsystem 1; bottom: acceleration-driven subsystem 2. Design value: L, low; M, medium; H, high; A, any.

	Subsystem 1		Subsystem 2		Whole system		Uniform damping	
	r	e	r	e	r	e	r	e
Low level	H	L	A	H	H	L	H	L
High level	A	H	L	L	A&eH	A&rL	L	L
Low level	M	M	L	H	A	M→H	A	M→H
High level	L	L	H	L	H	L	H	L

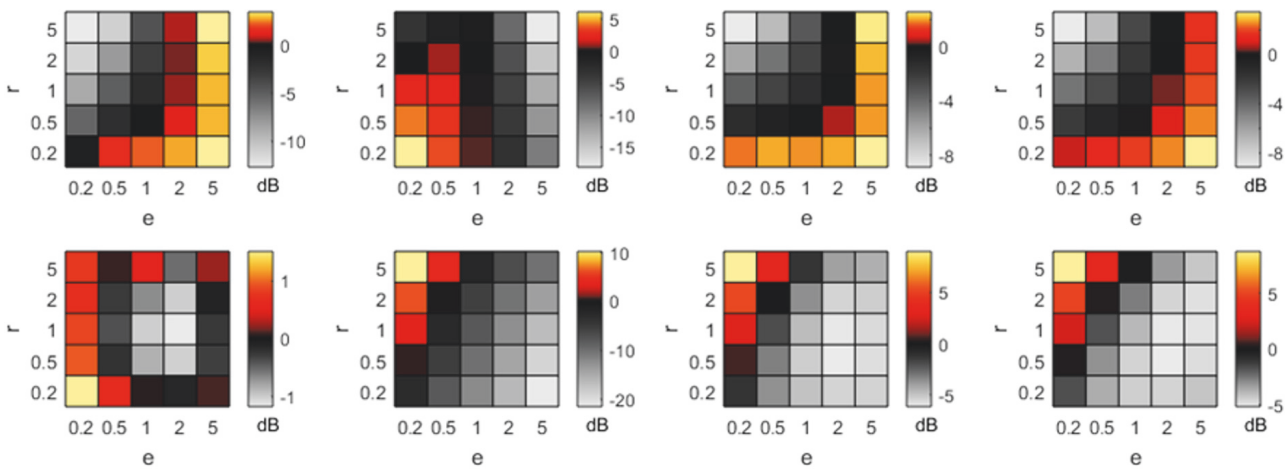

Figure 3: Normalised damping-averaged kinetic energy in dependence of resistance and eigenvalue ratios.

Table 1 provides the summary of relative vibration energy level values in dependence of design parameter values. For example, the combination of high resistance ratio and low ratio of natural frequencies gives low source vibration level of a system source-support but high housing vibration level of a system housing-equipment. The table can be thus considered as a simplified design chart regarding vibration transmission.

2.2. Coupling of Two Arbitrary Degrees of Freedom. If a system consists of multiple vibration modes, it is useful to analyse how does the kinetic energy of individual modes depend on damping. It will be assumed that the studied system consists of a source and a receiver coupled by an elastic connection of stiffness k. The terms source and receiver merely indicate that one subsystem is driving the other. A particular mode of each of the two subsystems is characterised by the mass-stiffness-damping triplet. Figure 4 illustrates the mechanical setup in the present analysis.

With two m, k, and η subsystems and the elastic connection coupling defined by its own k_c and η_c pair, there exist 8 independent system parameters. The objective is to assess the relative influence of damping of the source, receiver, and coupling on the kinetic energies involved. The model described in Appendix A can be likewise used in the present analysis provided that the source modal stiffness is added to the q_1 term. In this case, the symbol k_1 will refer to the stiffness of the elastic coupling.

The parameters can be now put in the nondimensional form similar to that used for the two-degrees-of-freedom system shown in Figure 1. As in the preceding section, the source and the receiver will be identified by the ratio of resistances r, the ratio of decoupled eigenvalues e, and the loss factors of the source and the receiver, η_s and η_r. The

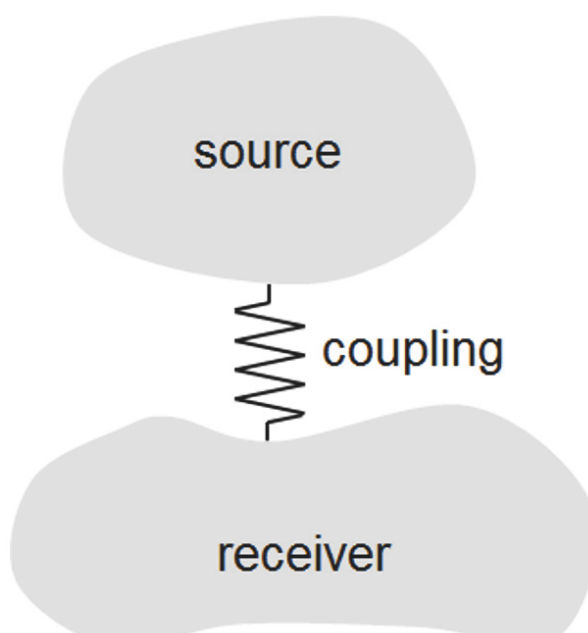

Figure 4: Coupling of two degrees of freedom.

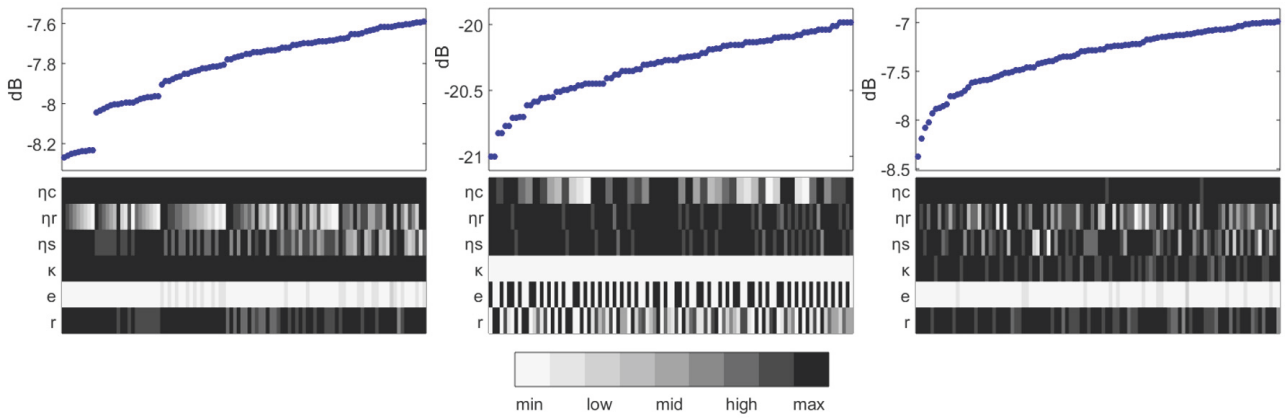

Figure 5: 100 lowest values of normalised kinetic energy level of a resiliently coupled system source-receiver. Left: source; middle: receiver; right: entire system.

presence of elastic coupling adds two new parameters: k_c and η_c. In order to convert the coupling stiffness k_c to a suitable nondimensional form, the coupling stiffness factor κ will be introduced, equal to the ratio of k_c and the geometric mean of the source and receiver stiffness:

$$\kappa = \frac{k_c}{\sqrt{k_s k_r}} \tag{2}$$

In analogy to the previously made analysis, each of parameters r, e, and κ was attributed 9 values distributed from 0.2 to 5 in logarithmic fashion. Likewise, each of three loss factors η_s, η_r, and η_c assumed the 9 values from 0.2% to 5%. The computation of kinetic energies was subsequently done for all of 531,441 possible combinations of parameter values.

Figure 5 shows the 100 lowest normalised kinetic energy levels of the source, receiver, and entire system in dependence of the 6 nondimensional parameters. The normalisation was done by subtracting from the computed levels the average level. The latter was obtained by applying an appropriate correction that took into account the nonlinear distribution of discrete parameter values. It can be seen that the lowest levels of the source are obtained if the following conditions are met: the receiver is of much higher resistance than the source, the source eigenfrequency is much higher than that of the receiver, and both the stiffness and the damping of the coupling are high. On the contrary, the receiver will get the lowest level if the coupling stiffness is low and if the damping of both the source and the receiver is high. The conditions of the global energy minimum are similar to these related to the source.

It is interesting to find out whether the effect of different system parameters on the energy level can be factorised, that is, represented in terms of individual parameters, independently from each other. This is presented in Figure 6. For each of the 6 parameters, the averaged parameter value is shown for 1-1000 lowest and 1-1000 highest energy levels. The averaging is done using the geometrical mean, considered to be more representative than the algebraic one. For example, the mean value of a given parameter Ψ averaged over n lowest energy levels reads $\overline{\Psi}_n = (\Psi_1 \ldots \Psi_n)^{1/n}$, where Ψ_1 is the Ψ value corresponding to the lowest level, Ψ_2 is the value corresponding to the next lowest level, and so forth. The averaged parameter values relative to the highest levels were obtained in the analogous way.

Table 2: Damping design parameters for low vibration level. Design value: L, low; M, medium; H, high.

	r	e	κ	η_s	η_r	η_c
Source	H	L	H	H	M	H
Receiver	M	M	L	H	H	M-H
System	H	L	H	H	M-H	H

Figure 7 shows the averaged normalised energy levels, lowest and highest, corresponding to averaged parameters given in Figure 6. It is seen that favourable parameter combinations can reduce the source level up to 7-8 dB and the receiver level up to 20 dB with respect to the mean level values. On the contrary, poor parameter combinations can increase the levels by more than 10 dB. These figures indicate that there exists room for effective damping use, where low-vibration design is concerned.

A condensed reading of Figure 6 is provided in Table 2, which can serve as a rough guideline to the selection of damping of coupled structures.

3. Vibration Damper

One way of vibration reduction of an elastic structure consists in applying point dampers, passive or active. Two issues equally matter where the damper needs to be optimised: its location on the structure and the value of its governing parameter(s).

In order to illustrate the nature of damper optimisation task, a simple demonstrator model, illustrated in Figure 8, will be employed. The receiver structure that needs controlling will be modelled as an elastic beam. In order to account for a realistic type of excitation, another beam will be provided to act as a vibration source of finite impedance. The source is driven by a combination force-moment. Its coupling

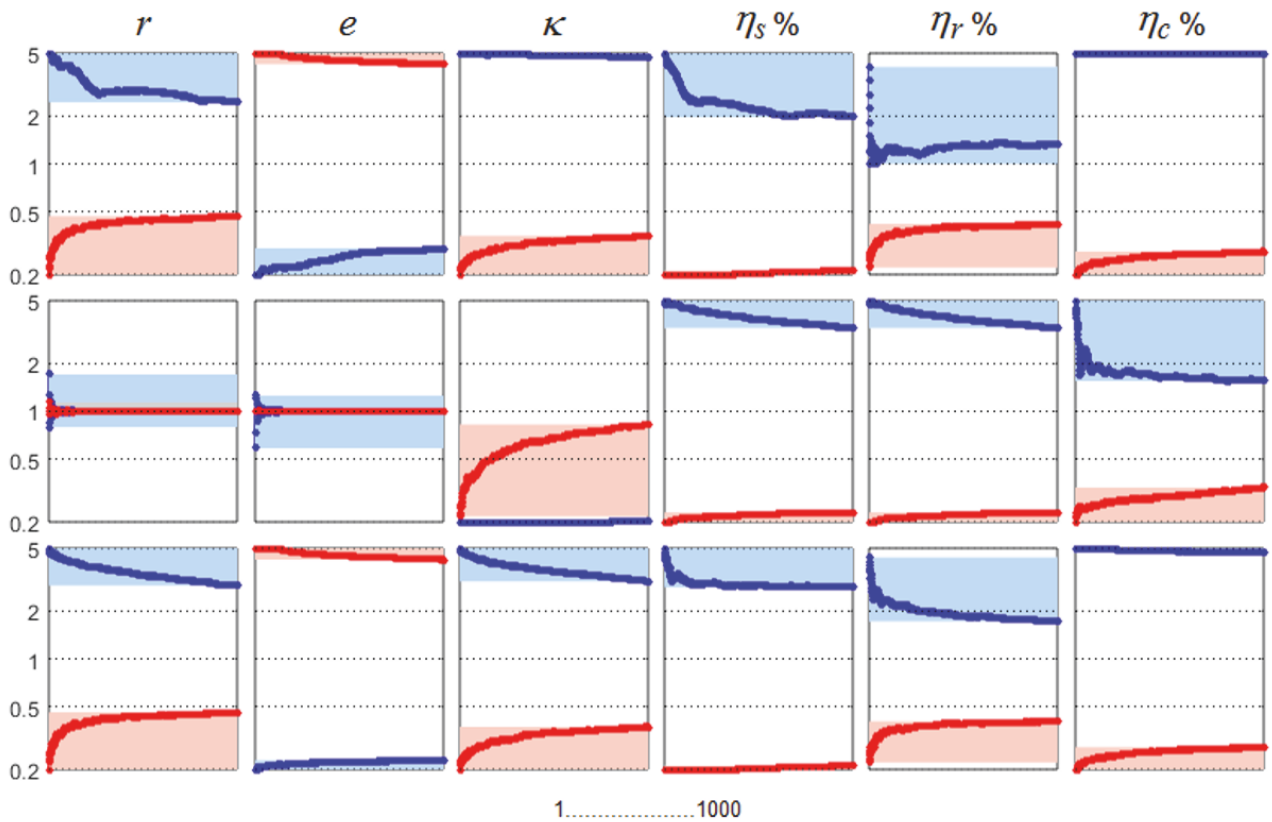

Figure 6: Average values of system parameters producing lowest (blue) and highest (red) levels of kinetic energy. Top: source; middle: receiver; bottom: entire system.

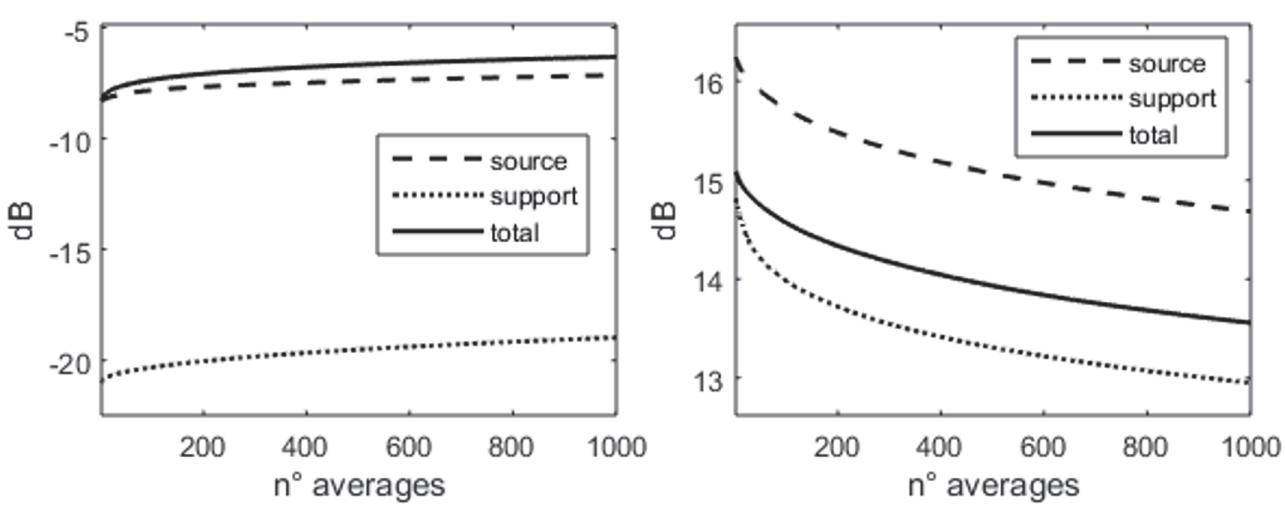

Figure 7: Average values of normalised levels of kinetic energy corresponding to parameters of Figure 6. Left: lowest levels; right: highest levels.

to the receiver is done by a resilient suspension composed of stiffness-mass-stiffness isolators. The suspension isolators possess both translational and rotational stiffness. The mathematical model of the system shown in Figure 8 is provided in Appendix B.

In the following examples, the kinetic energies within the system will be integrated within the 0-2 kHz range, considered to be sufficiently wide to provide enough insight into the role played by damping. The following parameters were selected:

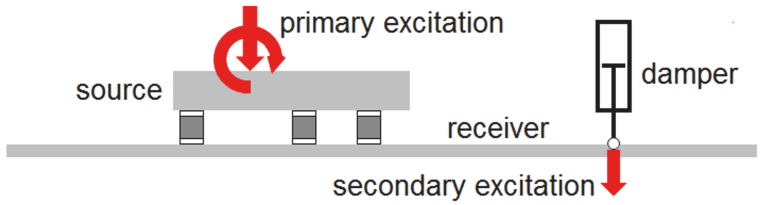

Figure 8: System source-receiver.

(i) Source beam: steel, length 0.4 m, width 7.5 cm, height 2.5 cm, loss factor 1%.

(ii) Stiffness per spring: in translation 50 N/mm and in rotation 20 kNm/rad.

(iii) Spring mass 0.1 kg and moment of inertia 0.02 kg m^2.

(iv) Receiver beam: aluminium, length 1.3 m, width 7.5 cm, height 2 cm, loss factor 1%.

In order to compute the kinetic energy T of the receiver, the following relationship that involves the total supplied power Π given in complex form will be used [4]:

$$T = \frac{\mathrm{Re}\{\Pi(1 - j\eta)\}}{2\eta\omega} \tag{3}$$

The complex form of power is an artefact. While its real part corresponds to the time-averaged (net) power, its imaginary part lacks any definite physical meaning. Nonetheless, the complex power is useful for computation in frequency domain. It is obtained by multiplying dynamical quantities, forces, and moments by the conjugate of corresponding kinematic quantities, translations, and rotations, where both groups of quantities are represented by complex amplitudes. Equation (3) applies to any linear structure.

Using the equations of the system with a damper, given in Appendix B, of the (complex) vibration power supplied to the receiver beam will be carried out as a first step. Once the value of the supplied power is known, the kinetic energy of the receiver is easily computed using (3). Cases with either passive or active dampers will be treated in this way.

3.1. Passive Damper. A purely viscous damper is taken to act in a single point of a clamped-clamped receiver beam driven by a free-free source beam via 3 resilient mounts. The damper is assumed to work in translation only. The source beam is coupled to the receiver beam by 3 mounts symmetrically positioned with respect to its centre. The combined excitation force-moment is offset by 0.15 m from the source centre. The source is offset by −0.2 m with respect to the receiver centre. The excitation spectrum is taken as constant or rising with frequency as indicated; the ratio between the excitation force and moment power spectra is kept constant, equal to $G_M/G_F = 0.04$ m^2 with a $\pi/2$ phase shift of the cross spectrum G_{MF}.

Figure 9 shows the spectral density of input power supplied by the source via the 3 mounts and of output power absorbed by the damper placed at 0.25 m from the receiver centre. It can be seen that at the selected position the damper efficiently absorbs energy close to resonance frequencies up to approx. 200 Hz. At higher frequencies, the absorption by the damper diminishes since the receiver itself absorbs more efficiently.

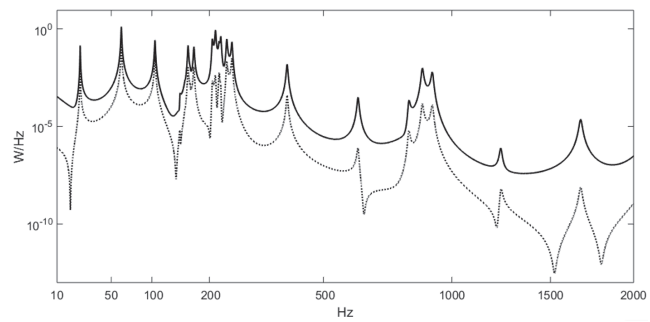

Figure 9: Power to the receiver: full line, supplied by the source; dotted line, absorbed by the damper.

Figure 10 shows the difference of vibration energy levels of the receiver beam with and without damper for a range of damper rate values and a range of damper positions along the beam. The energy levels were numerically integrated in the range of 0-2 kHz. Two upper plots refer to two different positions of the source substructure. The abscissa is adjusted to the length of the receiver beam and the coupling positions of the three springs are indicated by triangles on the top. The excitation position on the source beam is indicated by a red mark. The dotted line on each plot shows the value of damper rate producing maximum vibration reduction. This value has been obtained by using (1) with the condition $\partial T/\partial q = 0$, where q is damper rate. The force spectrum was taken as either flat or frequency-weighted. In some cases, the level difference is positive; this is indicated by warm tones. This implies that the damper may increase vibration if poorly tuned to the structure. While a passive damper will always consume power, its presence affects the power input by the primary source in such a way that the total power delivered to the structure may increase if the damper is present.

Several simple conclusions can be drawn from the displayed plots:

(i) A passive damper may lead to an increase of vibration if improperly positioned or adjusted.

(ii) On the contrary, a well-tuned damper can decrease the overall broadband vibration level by ≈10 dB (this applies to monodimensional structures; other

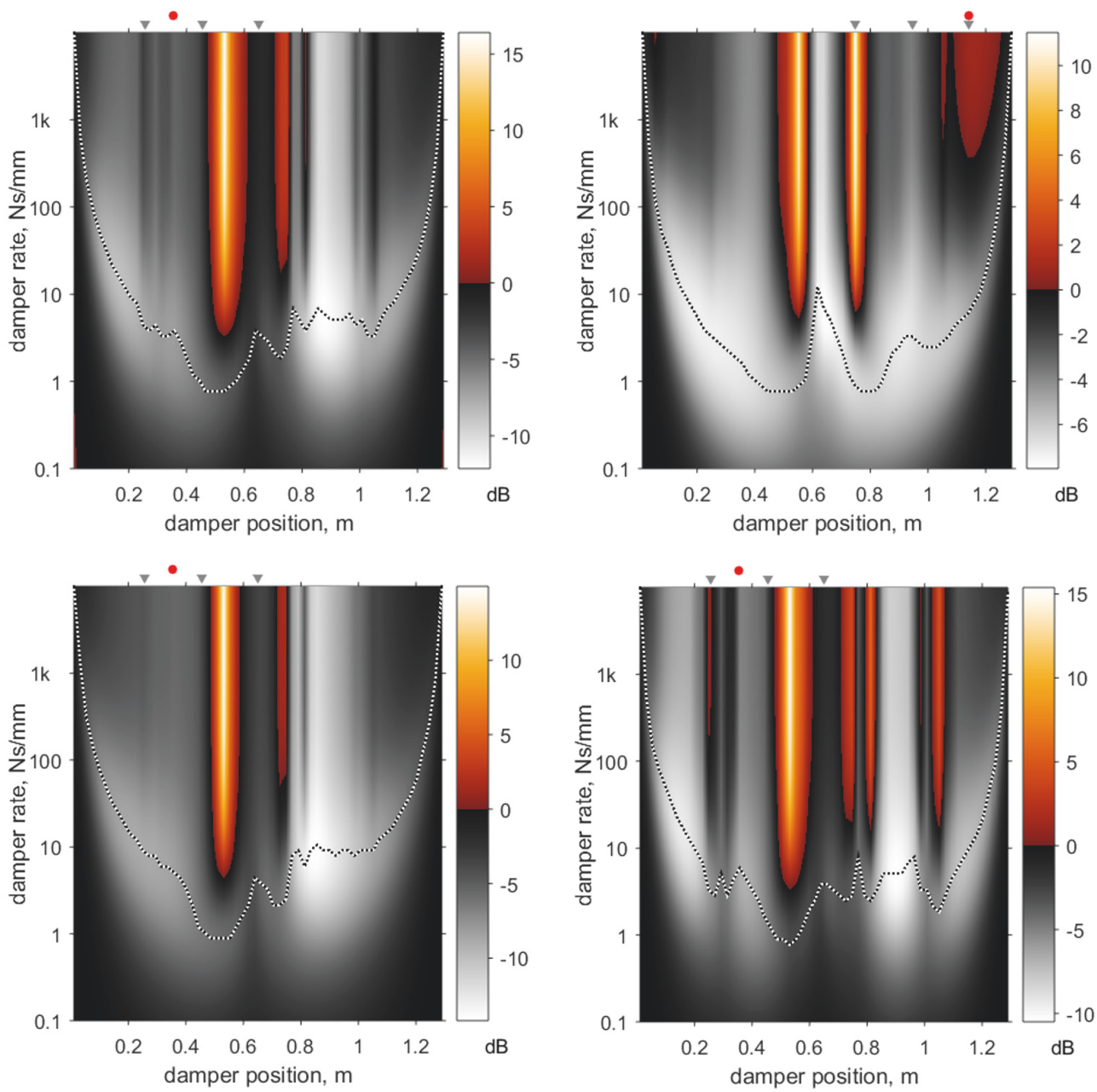

Figure 10: Kinetic energy level change of receiver beam by a passive damper. Excitation: top: $\propto \sqrt{f}$ RMS spectrum; bottom left: flat spectrum; bottom right: $\propto f$ spectrum. Dotted line: damper rate giving best energy reduction.

structures will need more dampers to achieve such a level of vibration reduction).

(iii) Optimum damper position is not necessarily close to the vibration source.

It should be pointed out that the optimum damper tuning in terms of both position and damping capacity is unlikely to be attainable in practice by computation only. A combination of measurement and modelling may lead to a solution close to the optimum. The idea is to measure vibration at representative positions of the targeted structure twice: (a) with the source operating and then (b) by impacting selected damper candidate points by impedance hammer. This procedure should theoretically suffice to indicate a suitable damper location and a correct damper rate.

3.2. Active Damper. The optimisation of a passive damper regarding a given damper position consists of finding the damper rate that minimises the selected cost function, the kinetic energy in the present study. The amplitude-phase relationship between the resistive force and the coupling velocity of a passive damper is independent of dynamic properties of the structure involved. Such a relationship makes the flow of energy always enter the damper.

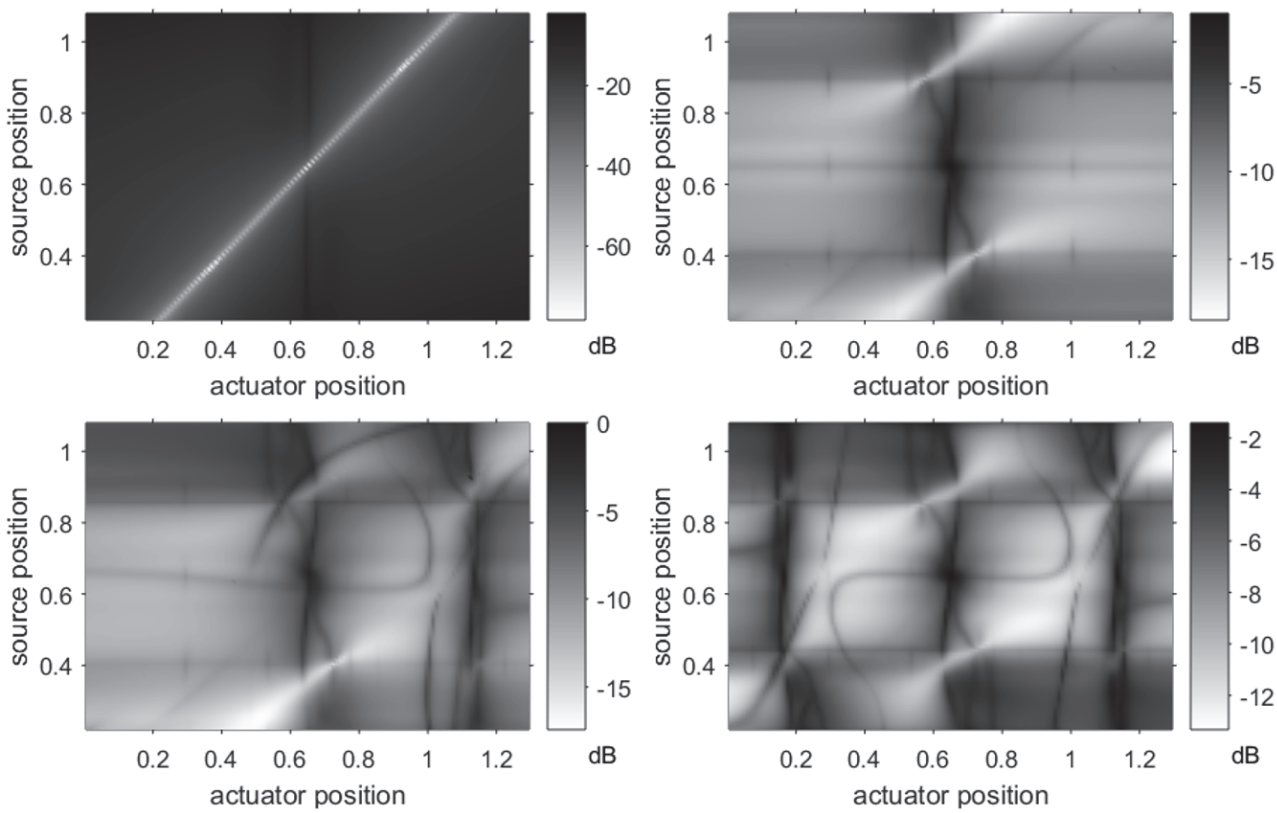

Figure 11: Drop in kinetic energy level of receiver beam due to an optimised active damper. Top: clamped-clamped receiver: left, single mount; right, 3 mounts. Bottom: 3 mounts: left, clamped-free receiver; right, free-free receiver. RMS excitation spectrum $\propto \sqrt{f}$.

An active damper (actuator), if properly adjusted, will produce a control force that does not necessarily absorb energy but may even deliver it to the structure. The phase relationship force-velocity will depend on both the dynamic properties of the receiver structure at the actuator's driving point and the way the structure is excited by own excitation. The optimum value of actuator force is thus frequency-dependent.

In the next examples, the actuator is supposed to create a normal force only. The optimum actuator force F_o can be obtained by setting the conditions $\partial T/\partial \Re F_o = 0$ and $\partial T/\partial \Im F_o = 0$ with $\Re$ and $\Im$, respectively, denoting real and imaginary parts. The value of F_o is evaluated in Appendix C.

The maps on Figure 11 show the decrease of kinetic energy level with the actuator operating. The system is the one from Figure 4. The variables appearing in the abscissa and the ordinate scale are the position of the actuator and the centre position of the source. The first map is for the case of a single mount of vanishing angular stiffness centrally positioned on the driving beam. The latter is driven by a force in its centre. This particular setup was selected to provide conditions very close to single force/no moment excitation on the receiver beam. In the latter case, the optimum position of actuator is exactly at the coupling position: the optimum tuning will make the actuator produce the same force as the spring but 180° opposite in phase. A huge drop of overall kinetic energy can be seen at the 45° line, where the actuator positions coincide with the source positions. In all other cases, such a specific pattern disappears; the optimum actuator position is not centred at the source. Reduction of energy levels of the order of 15 dB can be obtained if the source is close to the clamped end. Further analysis has shown that energy dissipation is efficient close to clamped ends, which results in an increased level of reduction.

An efficient control of a complex structure would need several actuators. High figures of reduction can be theoretically obtained using a single actuator but these apply to specific cases. For example, a 50 dB reduction of a single vibration mode under careful selection of actuator position was reported in [5]. Such high a figure cannot of course be attained where global broadband vibration of a multimodal system is concerned.

It has been assumed in this study that the actuator can deliver a pure force of prescribed amplitude and phase. In real applications, an actuator needs support; thus such an excitation is difficult to realise in practice. To overcome the problem, a supported actuator was proposed already half a century ago [6]. In [7], it was found that the performance of an inertial actuator in reducing power input to the vibrating plate was close to that of an equivalent impedance of the optimal active control system. Thus, it seems that solutions are available regarding the physical support of a vibration

actuator. The principal objective of this section, however, is not to focus on the actuator technology; it is rather to focus on the effect of an optimal actuator tuning on a receiver.

4. Conclusions

The present simple study shows that the potential of damping for the purpose of reduction of global vibration could be fully exploited if the position of damping treatment or of devices is chosen to match dynamic characteristics of the structures concerned. The subject is so wide that any methodical approach to it could not possibly fit a single paper; rather it was illustrated through simple demonstrations, where the reduction of global structural vibration was taken as a goal.

Some basic guidelines were established regarding the isolation of vibrations, principally in the lower frequency range. Rudimentary optimisation rules were obtained by multiparameter analysis that has revealed that optimum damping cannot be factorised out of the remaining dynamical parameters. It has been shown that the system parameters that lead to efficient reduction of the vibration level of a given subsystem are usually in conflict with those optimised for the other subsystem.

Point damping devices, such as passive or active absorbers, can be rather efficient if they were well tuned to the vibrating structure. It should be recalled that the role of an absorber is not to draw as much energy out of the structure as possible but to reduce its level as much as possible. The energy taken out of a vibrating structure by an ill-tuned damper may become overcompensated by that injected by the primary vibration source, owing to the coupling between the two. An optimum matching of a damper to a receiver structure thus requires a major design effort in order to enable correct identification of both the most suitable position and the optimum damper parameters.

Appendix

A. Kinetic Energy of a Double Oscillator

The Lagrangian L of the system in Figure 1 is composed of kinetic energy and potential energy T and V: $L = T–V$. Assuming no dissipation for the time being, the two energies read

$$T = T_1 + T_2 = \frac{m_1}{2}\dot{u}_1^2 + \frac{m_2}{2}\dot{u}_2^2$$
$$V = \frac{k_1}{2}(u_1 - u_2)^2 + \frac{k_2}{2}u_2^2 \tag{A.1}$$

with u denoting vibration displacement. The Lagrange's equations

$$\frac{d}{dt}\frac{\partial L}{\partial \dot{u}_n} - \frac{\partial L}{\partial u_n} = F_n \tag{A.2}$$

applied to the present system and transferred into frequency domain enable one to obtain the displacements of two masses as functions of frequency. The damping can now be included in the form of complex stiffness, $k = k_0(1 + j\eta)$, with k_0 denoting the real part of stiffness. Assuming broadband excitation, the spectral densities of kinetic energies T' of the two masses can be found to depend on the power spectral density of excitation in the following way:

$$T_n'(\omega) = \frac{m_n E_n}{D}, \quad n = 1, 2 \tag{A.3}$$

where

force excitation is

$$E_n = \beta_{F,n}\omega^2 G_F,$$
$$\beta_{F,1} = |q_2|^2, \tag{A.4}$$
$$\beta_{F,2} = |k_1|^2$$

and kinematic excitation

$$E_n = \beta_{a,n}\frac{|k_2|^2}{\omega^2}G_a,$$
$$\beta_{a,1} = |k_1|^2,$$
$$\beta_{a,2} = |q_1|^2 \tag{A.5}$$
$$q_1 = k_1 - m_1\omega^2,$$
$$q_2 = k_1 + k_2 - m_2\omega^2$$
$$D = 2\left|q_1 q_2 - k_1^2\right|^2$$

The symbols G_F and G_a stand for the force and acceleration power spectral densities of the source and base excitations, respectively. These two densities are functions of radian frequency ω. The damping is included in the usual way by making the stiffness k complex: $k = k_0(1 + j\eta)$, with k_0 denoting the real part of stiffness.

The total kinetic energy of subsystems 1 and 2 can be obtained by integration:

$$T_n = \int_0^\infty T_n'(\omega)\, d\omega, \quad n = 1, 2 \tag{A.6}$$

The integration was carried out numerically with a changing integration step in order to fit the large gradient of the function T' close to two minima of its denominator D, which are at the natural frequencies of the coupled system. At frequencies well above the higher of the two natural frequencies, the density T' can be safely approximated by its $\omega \to \infty$ asymptote, proportional to ω^{-b},$b > 0$. The numerical integration was here stopped at a frequency ω_l five times the higher natural frequency and the remaining integration from ω_l to infinity was done analytically.

B. Model of a Source-Receiver System

Both the source and receiver are modelled as finite beams vibrating in flexure. Each beam is modelled using Euler-Bernoulli equation of motion. The beam response for any

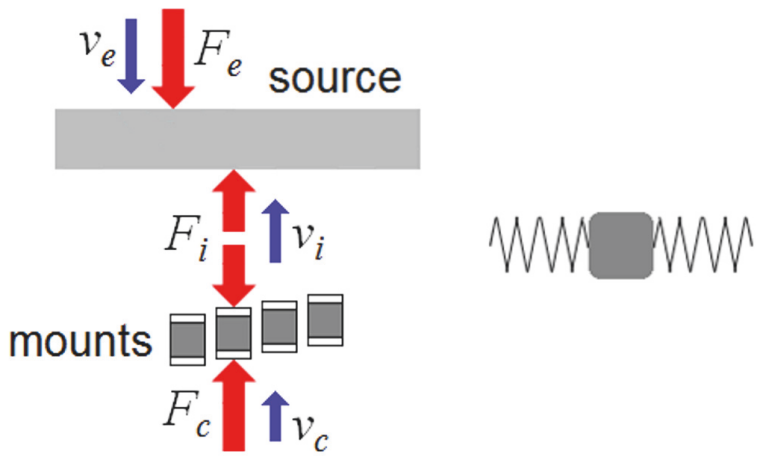

Figure 12: Left: assembled source. Right: mount model.

combination of free or clamped ends is obtained in closed form using wave approach. The details of this type of modelling will be omitted, considered to be known enough to readers.

It will be supposed that the source and the receiver are coupled in K points via resilient mounts. Since the two structures are straight beams, each coupling point will be assigned two degrees of freedom: a normal displacement and a rotation. Both the source and the receiver will be characterised by the respective mobility matrices relative to coupling points: source coupling mobility Y^s_{cc} and receiver coupling mobility Y^r_{cc}. At any given frequency, each of these mobilities is thus a $K \times K$ matrix. In addition, the source will be characterised by the free velocity vibration at the coupling points. This vibration takes place when the source is excited in uncoupled state.

For the sake of convenience, it will be useful to assemble the source beam and the mounts into one assembled source structure. In this case, the free ends of mounts should be taken as coupling points between the assembled source and the receiver. Figure 12 shows the assembly scheme. The forces and velocities are shown symbolically by arrows: each arrow schematically represents the entire set of either forces/moments or translation/rotation velocities acting at the interfaces between subsystems. The superposition applicable to linear systems yields the following constituent equations:

$$\begin{aligned} v_i &= Y^s_{ie} F_e + Y^s_{ii} F_i \\ -v_i &= Y^m_{ii} F_i + Y^m_{ic} F_c \\ v_c &= Y^m_{ci} F_i + Y^m_{cc} F_c \end{aligned} \tag{B.1}$$

In (B.1), Y stands for impedance matrix, v and F stand for vibration velocity and force vector, and the superscripts s and m denote source and mounts, respectively, while the subscripts e, i, and c denote excitation, interconnection, and coupling points, respectively. The mobility matrix of the mount system consisting of K mounts will be a diagonal matrix of K submatrices, one per mount. Each mount is modelled as a spring-mass-spring unit with hysteretic damping (Figure 12). Both translational and rotational spring stiffness and translational and rotational inertia are accounted for.

Upon setting $F_e = 0$, a matrix relationship can be obtained between the force vector F_c and the velocity vector v_c: $v_c = Y^{as}_{cc} F_c$. The matrix Y^{as}_{cc} thus represents the mobility matrix of the assembly source-mounts:

$$Y^{as}_{cc} = Y^m_{cc} - Y^m_{ci} \left(Y^s_{ii} + Y^m_{ii}\right)^{-1} Y^m_{ic} \tag{B.2}$$

Likewise, by setting $F_d = 0$, a matrix relationship can be obtained between the excitation force vector F_e and the velocity vector v_c: $v^{as}_{cf} = Y^{as}_{ce} F_e$. The transfer matrix Y^{as}_{ce} makes the link between the excitation and the velocity of free mounts connections:

$$Y^{as}_{ce} = -Y^m_{ci} \left(Y^s_{ii} + Y^m_{ii}\right)^{-1} Y^s_{ie} \tag{B.3}$$

Figure 13 shows the entire system source-receiver, where the term "source" stands for the assembly source-mounts defined at the coupling points with the receiver by the mobility Y^{as}_{cc} and the free velocity v^{as}_{cf}. The system is supposed to be excited by the assembled source and additionally by a damper placed at an arbitrary point. The damper is supposed to provide to the receiver a single normal force F_d; its normal velocity will be denoted by v_d. If the damper is passive, a simple viscous-type relationship will be used, $F_d = -Cv_d$, where C is damper rate 2×2 matrix. Since the damper is supposed to provide normal force, only the first element of C, c_{11}, will be different from zero. If an active damper is modelled, the force F_d will be considered independent of v_d.

The following constitutive equations apply to the system:

$$\begin{aligned} v_c &= v^{as}_{cf} + Y^{as}_{cc} F_c \\ -v_c &= Y^r_{cc} F_c + Y^r_{cd} F_d \\ v_d &= Y^r_{dc} F_c + Y^r_{dd} F_d \end{aligned} \tag{B.4}$$

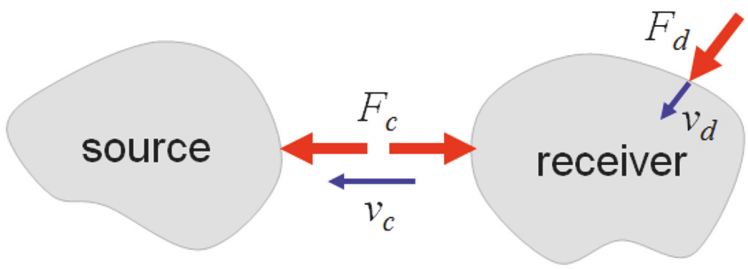

Figure 13: System source-receiver.

If a passive damper is attached having the damper rate matrix C, the vector of coupling forces F_c and the damper force vector F_d obtained from (B.4) read

$$\begin{aligned} F_c &= -\left[Y_{cc}^r + Y_{cc}^{as} - Y_{cd}^r \left(C + Y_{dd}^r\right)^{-1} Y_{dc}^r\right]^{-1} v_{cf}^{as} \\ F_d &= -\left(C + Y_{dd}^r\right)^{-1} Y_{dc}^r F_c \end{aligned} \tag{B.5}$$

Once the force vectors F_c and F_d have been computed, the associated velocity vectors v_c and v_d follow from (B.4). This makes it possible to compute the power entering the receiver beam. The input power consists of the component Π_c entering via the coupling points and the component Π_d leaving via the damper point:

$$\begin{aligned} \Pi_c &= \frac{1}{2}\left(F_c^* v_c\right)^*, \\ \Pi_d &= \frac{1}{2}\left(F_d^* v_d\right)^* \end{aligned} \tag{B.6}$$

where the asterisk denotes conjugate transpose. The known values of the powers Π_c and Π_d enable direct computation of kinetic energy of the receiver (see (3)).

C. Optimum Active Damper

The active damper should be optimised to minimise kinetic energy of the receiver. In such a case, the system equations (B.4) apply the same. However, the damper force F_d is not anymore simply a reaction between the receiver and the damper but it is controlled externally. The kinetic energy of the receiver has to be expressed as a function of the force F_d and the condition of minimum $\partial T/\partial \Re F_d = 0$ and $\partial T/\partial \Im F_d = 0$ is applied.

$$F_d = \frac{\alpha + j\beta}{\gamma} \tag{C.1}$$

The factors α, β, and γ are rather complex functions of system parameters:

$$\begin{aligned} \alpha &= \Re\left[\left(\lambda_1 + \lambda_2\right)\zeta\right], \\ \beta &= -\Im\left[\left(\lambda_1 - \lambda_2\right)\zeta\right], \\ \gamma &= \Re\left(\lambda_3 \zeta\right), \\ \zeta &= 1 + j\eta \\ \lambda_1 &= F_{sr}^* H, \\ \lambda_2 &= G^* v_{sr} + Y_{dc}^r F_{sr}, \\ \lambda_3 &= Y_{dd}^r - Y_{dc}^r G - G^* H \\ F_{sr} &= \left(Y_{cc}^{as} + Y_{cc}^r\right)^{-1} v_{cf}^{as}, \\ v_{sr} &= Y_{cc}^{as} F_{sr} - v_{cf}^{as}, \\ G &= \left(Y_{cc}^{as} + Y_{cc}^r\right)^{-1} Y_{cd}^r, \\ H &= Y_{cc}^{as} G \end{aligned} \tag{C.2}$$

Once the actuator force is identified, other system variables as well as the power supplied to the receiver can be obtained using (B.4) and (B.6).

Data Availability

The data used to support the findings of this study are available from the corresponding author upon request.

Conflicts of Interest

The author declares that there are no conflicts of interest regarding the publication of this paper.

References

[1] L. Cremer and M. Heckl, *Structure-Borne Sound*, Springer Berlin Heidelberg, Berlin, Heidelberg, 1973.

[2] C. T. Morrow, B. A. Troesch, and H. . Spence, "Random response of two coupled resonators without loading," *The Journal of the Acoustical Society of America*, vol. 33, pp. 46–55, 1961.

[3] A. T. Curtis and T. R. Boykin, "Response of Two-Degree-of-Freedom Systems to White Noise Base Excitation," *The Journal of the Acoustical Society of America*, vol. 33, no. 5, pp. 655–663, 1961.

[4] G. Pavic, "The role of damping on energy and power in vibration systems," *J. Sound Vib*, vol. 281, pp. 45–71, 2005.

[5] J. Keir, N. J. Kessissoglou, and C. J. Norwood, "An analytical investigation of single actuator and error sensor control in connected plates," *Journal of Sound and Vibration*, vol. 271, no. 3-5, pp. 635–649, 2004.

[6] T. H. Rockwell, "Investigation of Structure-Borne Active Vibration Dampers," *The Journal of the Acoustical Society of America*, vol. 38, no. 4, pp. 623–628, 1965.

[7] L. Benassi and S. J. Elliott, "Global control of a vibrating plate using a feedback-controlled inertial actuator," *Journal of Sound and Vibration*, vol. 283, no. 1-2, pp. 69–90, 2005.